Research article

Analysis of adaptive molecular mechanisms in response to low salinity in antennal gland of mud crab, *Scylla paramamosain*

Nan Mo [a], Tianyi Feng [a], Dandan Zhu [a], Jiaxin Liu [a], Shucheng Shao [a], Rui Han [a], Wentao Lu [a], Pingping Zhan [a], Zhaoxia Cui [a,b,*]

[a] *School of Marine Sciences, Ningbo University, Ningbo, 315020, China*
[b] *Laboratory for Marine Biology and Biotechnology, Qingdao National Laboratory for Marine Science and Technology, Qingdao, 266071, China*

A R T I C L E   I N F O

A B S T R A C T

As an important marine aquaculture species, the mud crab (*Scylla paramamosain*) is a good candidate for studying the osmoregulatory mechanism of crustaceans. While previous studies have focused on the osmoregulatory function of the gills, this study aims to explore the osmoregulatory function of the antennal glands. By the comparative transcriptomic analysis, we found the pathways of ion regulation including "proximal tubule bicarbonate reclamation" and "mineral absorption" were activated in the antennal glands of the crabs long-term dwelling in low salinity. The enhanced ionic reabsorption was associated with up-regulated ion transport genes such as *NKA*, *CA-c*, *VPA*, and *NHE*, and with energy metabolism genes such as *MDH*, *SLC25*, and *PEPCK*. The upregulation of *NKA* and *CA-c* was also verified by the increased enzyme activity. The lowered osmolality and ion concentration of the hemolymph and the enlarged labyrinth lumen and hemolymph capillary inside the antennal glands indicated the infiltration of external water and the responsively increase of urine excretion, which explained the requirement of enhanced ionic reabsorption. To further confirm these findings, we examined the change of gene expression, enzyme activity, internal ion concentration, and external ion concentration during a 96 h low salinity challenge with seven intervals. The results were basically consistent with the results as shown in the long-term low salinity adaptation. The present study provides valuable information on the osmoregulatory function of the antennal glands of *S. paramamosain*. The implication of this study in marine aquaculture is that it provides valuable information on the osmoregulatory mechanism of mud crabs, which can be used to improve their culture conditions and enhance their tolerance to salinity stress. The identified genes and pathways involved in osmoregulation can also be potential targets for genetic selection and breeding programs to develop more resilient mud crab strains for aquaculture.

1. Introduction

Salinity is an abiotic environmental factor that affects the basic biological processes of many aquatic crustaceans [1,2]. A sudden change in salinity may result in disruption of hemolymph osmolality and ion channel activity, resulting in slow growth, suppressed

immune response, and high mortality [3,4]. Monitoring and management of salinity is therefore one of the routine practices in crustacean aquaculture [5,6]. In recent years, climate change and the urbanization of coastal regions have brought great challenges to the salinity management in crustacean aquaculture [7,8].

In aquatic crustaceans, osmolarity plays a crucial role in this process. Some crustaceans could adapt to salinity change via a series of physiological and biochemical adjustments [9,10], such as neuroendocrine regulation [11,12], hemolymph ion regulation [13,14], and metabolic reprogramming [15]. Osmoregulation is the process of maintaining salt and water balance across membranes within the body, and involves the absorption or excretion of ions between the ambient medium and the body fluid through multiple organs such as gills and antennal glands [16,17].

The gills, especially the posterior region, are the main sites of gas exchange, osmoregulation and ion-regulation and are the key osmoregulatory organs in crustaceans [[18,19,38]]. It has been suggested that the gills have the ability to rapidly regulate hemolymph osmolality by altering the expression patterns of underlying candidate genes to tolerate large salinity fluctuations [[20–23]]. As salinity changes, candidate genes immediately respond by altering their expression patterns to counteract its adverse effects [[24–28]].

The antennal gland, also known as the green gland, is specialized excretory organs found in crustaceans [29,30]. They play a crucial role in osmoregulation, which is the maintenance of the balance of water and electrolytes in the body [[31–33]]. Different crustaceans use antennal glands to regulate ions differently [34,35]. The antennal gland of crustaceans has been viewed as a structural analogue of the mammalian kidney, consisting of a labyrinth and coelomosac, the labyrinth containing ion regulatory cells similar to the proximal tubules of the mammalian kidney [36]. Previous studies showed that the antennal gland contains at least two cell types, the coelomic cell (COE) and the labyrinthine cell (LBR) [37]. Previous reports have highlighted that the antennal gland is likely to be the organ responsible for adaptation in crabs, as it is known to have distinct functions such as: regulation of salt balance, excretion of waste products, maintenance of water balance, and osmoregulation in different environments [38,39]. For example, the chemotaxis of the Dungeness crab *Cancer magister* is regulated by the active absorption of Na^+, K^+, Ca^{2+}, Cl^- and HCO_3^- from the urine through the antennal glands to the osmotic pressure [31]. Similarly, antennal glands have been found in *Ocypode quadrata*, *Procambarus blandingi*, with dual functions of reabsorption and secretion [29 [40,41]]. The process of ion transport is regulated by carbonic anhydrase (CA) and Na^+/K^+-ATPase (NKA) in the tubular cells of the antennal glands [37 [42–45]]. However, details of the morphology and function of the antennal glands in brachyurans remain unclear due to their small size and difficulty in sampling.

The mud crab, *Scylla paramamosain*, is an euryhaline marine crab species that inhabits brackish and seawater in estuaries with salinity ranges of 5–33 ‰ [46,47]. The aquaculture of *S. paramamosain* is widespread in the coastal regions of south-east China [48, 49]. *S. paramamosain* exhibits a relative high tolerance to the salinity fluctuation [[50–52]], which makes it a good candidate for studying the osmoregulatory mechanism. Therefore, the aim of this study was to explore the regulatory transport mechanism of antennal glands under salinity changes by comparing histological changes, osmoregulation-related enzyme activities, and candidate gene expression patterns of long-term residence in low-salinity environment and short-term salinity stress environment.

2. Materials and methods

2.1. Animals and sample collection

For the study long-term salinity adaptation, 12 adult *S. paramamosain* (100.0 ± 5.0 g, mean ± S.D.) were acquired for the collection of tissue samples and construct cDNA libraries. Crabs of the 5 ‰ group were long-term dwelling in the 5 ‰ sea (Cixi, China, 30°02′–30°24′N, 121°02–121°42′E) and crabs of the 23 ‰ group were long-term dwelling in the 23 ‰ sea (Xiamen, China, 24°23′–24°54′N, 117°53–118°26′E). At the beginning of the experiment, 6 crabs were selected as biological replicates in each experimental group. The crabs used for the study were reared from larvae/juveniles at a mud crab semi-intensive free-range farm.

The acute low salinity trial was carried out in indoor rectangular blue rectangular covered tanks (40 × 30 × 20 cm, L: W: H) in the Laboratory of Crustacean Genomics and Molecular Genetics, Ningbo University, Ningbo, China. 120 adult crabs used for the acute low salinity trial were obtained from a crab farm with a salinity of 23 ‰ in Xiamen, China. All the crab was stocked in 20 L tanks containing aerated seawater (salinity 23 ‰, pH 7.2) and acclimated to the laboratory culture condition for 14 days beforehand. During the acclimation, the brackish water was maintained at salinity 23 ‰, pH 7.2, temperature 24 ± 1 °C, and dissolved oxygen 6 ± 0.5 mg/L; the animals are fed twice a day with clam meat. When the experiment began, 60 crabs (sex ratio 1:1) were transferred from the salinity of 23 ‰–5 ‰; meanwhile, the other 60 crabs were maintained at the salinity of 23 ‰ as the control group. The acclimation medium of 5 ‰ salinities was maintained and changed every 24 h, using a salinity meter to measure. In 0 h (10 min), 3 h, 6 h, 12 h, 24 h, 48 h, 72 h, and 96 h, 6 crabs were randomly selected for sampling at each time point as biological replicates. The survival rate was surveyed at the end of experiment.

Experimental design is to carry out RNAseq on long-term samples, and then carry out acute salinity stress experiment on 23 ‰ crabs in long-term experimental control group to detect physiological and biochemical indexes and mRNA expression. The antennal gland is located at the base of the eyestalk near the insertion of the second antenna, the superior aspect of the stomach, as 1 pair of oval sacs, opening at the base of the second antenna, consisting of a gland and a bladder. After the crab has been anesthetized on ice for 5 min and sacrificed by the destruction of the dorsal ganglia, it is kept on ice during the dissection procedure, the back is shelled, and after the gastric tissue has been removed, the position of the antennal glands is visualized and they are removed by forceps. For each group, the whole antennal gland of each crab was assigned for RNA extraction, protein extraction and microscopic studies, and hemolymph was drawn for osmolarity measurements. All animals were handled following the standard procedures of the Guide for the Use of Experimental Animals of Ningbo University.

2.2. The construction and analysis of transcriptomes

Total RNA (more than 2 μg) of the antennal glands of each crab was extracted following the method as described by Du et al. [53]. After enrichment and purification by the poly-T oligo-attached magnetic beads, the first-strand cDNA was synthesized by reverse transcriptase and random primers using the templates of artificially cleaved mRNA fragments. Next the second-strand cDNA was synthesized by DNA Polymerase I and RNase H. After purification and PCR amplification, the cDNA library was sequenced by the BGISEQ-500 sequencer (BGI, Shenzhen, China). The pair-end read length is 100.

The high-quality clean reads were generated by removing the adaptors, low-quality sequences (<Q20) and the sequences shorter than 50 bp of the RNA-Seq raw data using Solexa QA [54]. The differential gene expression analysis was pairwise comparison by DESeq2 [55] after the alignment of clean RNA-Seq reads onto the genome of *S. paramamosain* (GWHALOH00000000) using the HISAT2 package [56]. A gene with an adjusted P-value less than 0.05 and a fold change greater than 2 was defined as a differentially expressed gene. Gene annotation was conducted using the database of NR [57], GO [58], and KEGG [59]. Thereafter, GO enrichment and KEGG enrichment of the differentially expressed transcripts were analyzed using the R ClusterProfiler 4.0 with a P value of 0.05.

2.3. Real-time quantitative polymerase chain reaction (RT-qPCR)

Twelve DEGs in the transcriptome were selected for verification using qRT-qPCR to confirm the dependability of the transcriptome results. The same samples were used for both BGISEQ-500 sequencing and qRT-PCR validation. Total RNA of the antennal glands was extracted using the TRIzol reagent (Invitrogen, Carlsbad, US). The quantity and quality of RNA were determined by the NanoDrop 2000 micro-volume spectrophotometry (Thermo Fisher Scientific, Waltham, US) and the agarose gel electrophoresis, respectively. The cDNA was synthesized using the template of 2 μg extracted RNA by the PrimerScript™ RT reagent kit with gDNA Eraser (Perfect Real Time) (Takara Biotechnology, Kusatsu, Japan). RT-qPCR was carried out in the ABI 7500 real-time PCR system (Applied Biosystems, Foster City, US) following the program of 95 °C for 30 s, 32 cycles of 94 °C for 5 s, 55 °C for 30 s, and 72 °C for 10 s. All samples were run in triplicate, and each assay was repeated three times. For the standard curves of each gene, the amplification efficiencies were 95–105 % and the coefficient (R^2) were $0.98 < R^2$. The relative gene expression was calculated using the $2^{-\Delta\Delta Cq}$ method as described by Schmittgen and Livak [60], where the *β-actin* of *S. paramamosain* was used as the reference gene.

2.4. The measurement of osmolality and ion concentration

For each crab, 2 mL hemolymph was collected at the base of the third walking limb using a heparinized (100 IU/mL) syringe. The cells in hemolymph were removed by centrifugation (1000 g, 10 min, 4 °C). The hemolymph was firstly prepared using a T10B homogenizer (IKA, Staufen, Germany) following the method of Yao et al. [49]. The supernatant was collected after the hemolymph was centrifuged at 12,000 rpm for 20 min at 4 °C. The osmolality was analyzed using a Fiske 210 osmometer (Advanced Instruments, Norwood, US). The concentrations of Na^+, Cl^-, K^+, Ca^{2+}, and Mg^{2+} were measured using the commercial reagent kits (Jiancheng Bioengineering Institute, Nanjing, China) and the following method described by Long et al. [61]. The absorbance wavelength was set to 620, 480, 440, 610, and 540 nm on a SpectraMax M2 microplate reader (Molecular Devices, California, US) for measuring Na^+, Cl^-, K^+, Ca^{2+}, and Mg^{2+}, respectively.

2.5. Enzyme linked immunosorbent assay (ELISA)

The whole antennal glands (about 0.1 g) were homogenized in PBS (w: v = 1: 9) before being centrifuged (3000 rpm, 10 min, 4 °C). The enzyme activities of CA-g and NKA in the supernatant were analyzed using the commercial ELISA kits (Qiaodu Biomart, Shanghai, China) following the instruction of manufacturer. Briefly, 50 μL diluted sample and 100 μL HRP conjugates were mixed in an antibody pretreated microplate well. After incubated for 60 min at 37 °C, the plate was thoroughly washed five times by the wash solution. Later, 50 μL chromogen solution A and 50 μL chromogen solution B were added to each well and gently mixed. After incubated for 15 min at 37 °C in the dark, 50 μL stop solution was added and the optical density (O.D.) was measured at wavelength 450 nm using the SpectraMax M2 microplate reader (Molecular Devices, California, US).

2.6. Histology and transmission electron microscopy (TEM)

Three whole antennal glands were fixed in the 0.1 M phosphate buffer (Na_2HPO_4, NaH_2PO_4) containing 4 % paraformaldehyde for histology and in the 0.1 M PB containing 2.5 % glutaraldehyde (in 0.1 M phosphate buffer) for 4–6 h at 4 °C for TEM. The osmolality of the fixative solution was adjusted to 950 mOsm/kg to prevent cell shrinkage/swelling. To prepare histological slides, fixed tissue samples were firstly embedded into the paraffin block after a series of washing and ethanol dehydration. At the region of interest, 5-μm thick sections were transverse sliced using a KD-2268 microtome (Kedee, Jinhua, China) and then mounted on adhesive glass slides. After paraffin removal by xylene and a series of ethanol dehydration, the slide was H&E stained and sealed by nail polish around the coverslip. Histological pictures were taken using an OLYMPUS DP72 optical microscope (Olympus, Tokyo, Japan). For TEM, after rinsing with 0.1 M PB three times (15 min each), the tissues were fixed in 1 % OsO_4 overnight. After a series of washes and later ethanol dehydration, the tissue blocks were cleared by propylene oxide and embedded in Epon 812 resin. Ultrathin sections (50–70 nm thick) were cut with a diamond knife (DiATOME, Nidau, Switzerland) on a RMC PT-XL ultramicrotome (Boeckeler Instrument, Tucson, US) and then mounted onto 200-mesh copper grids. The air-dried grids were stained with 3 % uranyl acetate solution for 30 min and 6 %

lead citrate for 5 min prior to the observation by a Hitachi H-7650 transmission electron microscope (Hitachi, Tokyo, Japan) operating at 80 KV. The samples were assayed in triplicate and the experiments were performed in triplicate. All samples were assayed in triplicate and the sections done in triplicate.

2.7. Statistical analysis

After checking for normality and homogeneity of variance, data were subjected to a one-way ANOVA. If a significant main effect was detected, differences among treatment means were compared using Duncan's multiple range test. All data are presented as the means ± standard deviation (mean ± SD). The level of significance was set at $p < 0.05$. All analyses were performed using SPSS 18.0.0 for Windows.

3. Results

3.1. The comparative analysis of transcriptomes

Six cDNA libraries (three for each group) of antennal glands were successfully constructed, containing an average of 83,718,424 ± 1,124,465 good quality clean reads (Q20: 98.74 ± 0.10 %). The GC content of clean reads was 45.19 ± 0.45 % and the mapping rate to the genome was 76.92 ± 3.53 % (Table 1). There were 2507 differentially expressed genes (DEGs) between the group of 23 ‰ (1202 up-regulated) and 5 ‰ (1305 up-regulated) (Fig. 1A). Based on DEGs, the transcriptomes of four individual samples were clustered together for each experimental group (Fig. 1B). It demonstrated the transcriptomic similarity between samples within the same group and the transcriptomic variance between two groups.

Based on the GO annotation, most DEGs were involved in the subcategories of "binding" (44.65 %) and "catalytic activity" (36.56 %) of the category "molecular function", the subcategories of "cellular processes" (26.47 %) and "metabolic processes" (22.81 %) of the category "biological process", and the subcategories of "cells" (17.09 %), "cell part" (17.01 %), "membrane" (16.34 %), "membrane part" (15.16 %) and "organelles" (12.48 %) of the category "cellular component" (Fig. S1A).

The top KEGG pathways enriched by DEGs were related to the processes of ion regulation ("proximal tubule bicarbonate reclamation" and "mineral absorption"), hormone production ("steroid hormone biosynthesis", "salivary secretion", "glycolysis/gluconeogenesis" and "bile secretion"), signal transduction ("phosphatidylinositol signaling system", "cAMP signaling pathway", and "adrenergic signaling in cardiomyocytes"), and metabolism ("pyrimidine metabolism", "purine metabolism", "protein digestion and absorption" and "glutathione metabolism") (Fig. S1B).

3.2. The DEGs related to osmoregulation

Compared with the 23 ‰ group, the up-regulated genes in the 5 ‰ group consisted of Na^+/K^+-ATPase (*NKA*), V-type proton (H^+)-ATPase (*VPA*), cytoplasmic carbonic anhydrase (*CA-c*), adenylate cyclase (*AC*), ATP-binding cassette subfamily C (*CFTR*), solute carrier family 25 (*SLC25*), malate dehydrogenase (*MDH*) and phosphoenolpyruvate carboxykinase (*PEPCK*), while the down-regulated genes were solute carrier family 1 (*NBC1*), sodium/hydrogen exchanger (*NHE*), glycosyl-phosphatidylinositol-linked carbonic anhydrase (*CA-g*), and succinate dehydrogenase (*SDH*) (Table 2; Fig. 2A). The results of qRT-PCR confirmed that *NKA*, *VPA*, *CA-c*, *AC*, *PEPCK*, *SLC25*, *MDH*, and *CFTR* were higher expressed in the 5 ‰ group than the 23 ‰ group, and the expression of *NBC1*, *NHE*, *CA-g*, and *SDH* in the 5 ‰ group were lower than those in the 23 ‰ group (Fig. 2B). The primers used for RT-qPCR are listed in Table 3.

### 3.3. The long-term adaptive responses to the low salinity

To adapt to the low salinity environment, the hemolymph osmolality of 5 ‰ group was lowered to 651.0 ± 166.3 mOsm/kg in comparison to 851.2 ± 33.8 mOsm/kg of the 23 ‰ group (Fig. S2A). As the major ionic components in the hemolymph, the concentration of Na^+, Cl^-, Ca^{2+}, Mg^{2+} and K^+ dropped from 359.4 ± 2.8 to 204.5 ± 4.7 mmol/L (Fig. S2B), 231.1 ± 3.2 to 194.5 ± 5.5 mmol/L (Fig. S2C), 10.3 ± 0.1 to 8.6 ± 0.5 mmol/L (Fig. S2E), 10.9 ± 0.3 to 8.2 ± 0.1 mmol/L (Fig. S2F), and 7.1 ± 0.3 to 3.4 ± 0.2 mmol/L (Fig. S2D), respectively. The decreasing concentration of the major hemolymph ions were consistent with the lowered hemolymph osmolality.

As the key enzymes for ion transport, the enzyme activities of CA-c (Fig. 3A) and NKA (Fig. 3B) in the antennal glands increased in the 5 ‰ group compared with the 23 ‰ group. This result was also consistent with the upregulated mRNA expression of *CA-c* and *NKA*

**Table 1**
The basic information of constructed transcriptomes.

Category	23 ‰_1	23 ‰_2	23 ‰_3	5 ‰_1	5 ‰_2	5 ‰_3
Raw reads	84,606,380	84,572,236	84,595,532	84,422,116	87,402,194	84,610,176
Clean reads	83,515,976	83,278,856	83,081,644	83,196,180	85,995,136	83,242,754
Q20 (%)	98.81	98.70	98.73	98.83	98.55	98.79
GC content	45.33	45.50	45.87	44.81	44.80	44.83
Mapping rate (%)	78.12 %	77.94 %	77.34 %	77.34 %	79.40 %	78.86 %
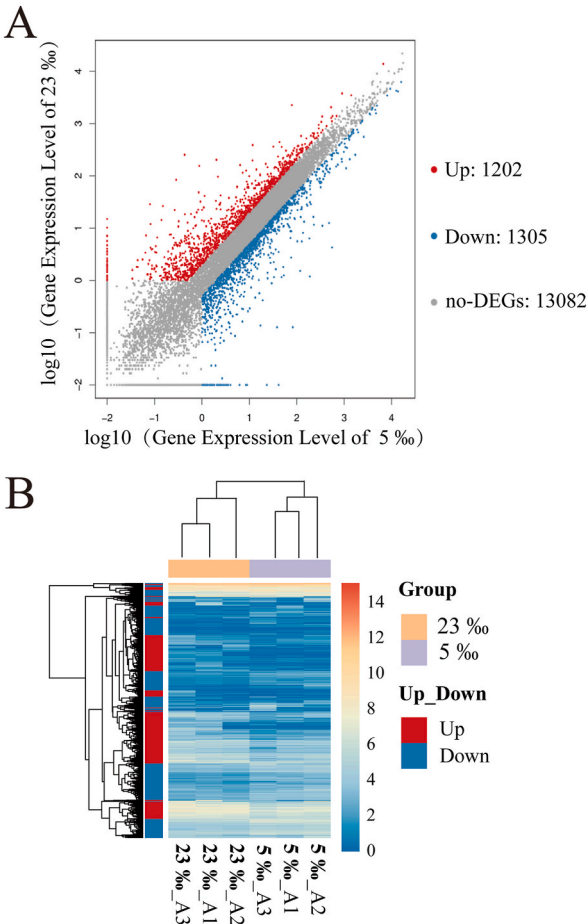
Fig. 1. Differentially expressed genes (DEGs) of transcriptomes between 5 ‰ and 23 ‰ group. A, a volcano plot showing the relative expression levels of all DEGs; B, a heatmap showing the clustering of all transcriptomic samples based on DEGs.

Table 2
The list of differentially expressed genes involved in osmoregulation.

Gene name	Gene ID	Annotation	Mean of RPKM	
			5 ‰	23 ‰
NBC1	nixue_GLEAN_10,003,375	Solute carrier family 1 [*Metaseiulus occidentalis*]	8.62 ± 3.51	18.89 ± 8.71
NKA	nixue_GLEAN_10002718	Na^+/K^+-ATPase [*Portunus trituberculatus*]	66.37 ± 25.70	32.58 ± 12.47
NHE	nixue_GLEAN_10010144	Sodium/hydrogen exchanger [*Monomorium pharaonis*]	6702.89 ± 2334.24	13872.48 ± 2790.12
VPA	nixue_GLEAN_10013828	V-type proton (H^+)-ATPase [*Nephrops norvegicus*]	41.22 ± 25.60	19.82 ± 0.65
CA-g	nixue_GLEAN_10017623	Glycosyl-phosphatidylinositol-linked carbonic anhydrase [*Biomphalaria glabrata*]	9.44 ± 1.20	62.12 ± 2.90
CA-c	nixue_GLEAN_10012647	Cytoplasmic carbonic anhydrase [*Eptatretus stoutii*]	2.71 ± 0.50	0.89 ± 0.10
AC	nixue_GLEAN_10015843	Adenylate cyclase [*Capitella teleta*]	7.05 ± 4.30	3.22 ± 1.08
CFTR	nixue_GLEAN_10015378	ATP-binding cassette, subfamily C (CFTR/MRP) [*Vollenhovia emeryi*]	129.22 ± 69.51	46.32 ± 31.12
SLC25	nixue_GLEAN_10002477	Solute carrier family 25 [*Scylla olivacea*]	1976.75 ± 881.26	684.16 ± 379.12
PEPCK	nixue_GLEAN_10009777	Phosphoenolpyruvate carboxykinase [*Nephrops norvegicus*]	1564.06 ± 409.00	759.44 ± 282.53
MDH	nixue_GLEAN_10013823	Malate dehydrogenase [*Crassostrea gigas*]	1283.72 ± 400.90	492.08 ± 76.10
SDH	nixue_GLEAN_10008857	Succinate dehydrogenase [*Sarcophilus harrisii*]	79.12 ± 46.76	162.15 ± 20.50
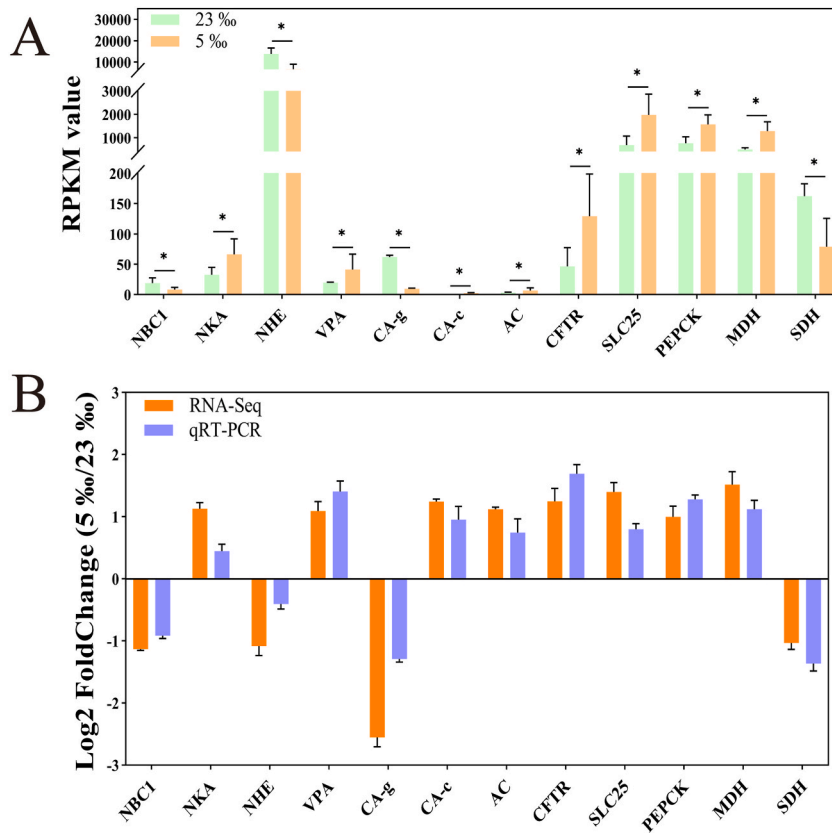
Fig. 2. The comparison of gene expression for the osmoregulation related DEGs. A, the comparison of gene expression magnitude (RPKM) of DEGs. B, the confirmation of differentiated gene expression by qRT-PCR. *NBC1*, Solute carrier family 1; *NKA*, Na^+/K^+-ATPase; *NHE*, sodium/hydrogen exchanger; *VPA*, V-type proton (H^+)-ATPase; *CA-g*, glycosyl-phosphatidylinositol-linked carbonic anhydrase; *CA-c*, cytoplasmic carbonic anhydrase; *AC*, adenylate cyclase; *CFTR*, ATP-binding cassette, subfamily C; *SLC25*, solute carrier family 25; *PEPCK*, phosphoenolpyruvate carboxykinase; *MDH*, malate dehydrogenase; *SDH*, succinate dehydrogenase. Bars in the diagrams represent the mean ± SD, and statistically significant difference ($P < 0.05$) is indicated by an asterisk (*).

in the 5 ‰ group (Table 2 and Fig. 2A).

The sectioning level is crossed by the anterior part and includes both the proximal tubular region and the distal tubular region. The distal tubular region of the antennal gland contains tubular cells and a large coelomosac. There was an intermittent separation of hemolymphatic spaces between the coelomosac and the labyrinth cells of the tubular-lining labyrinth cells. Hemolymph vessels are found in the proximal tubular region of the antennal gland and is the entrance for the coelomosac artery.

LBRs are cuboid cells with apical brush-boarder microvilli, basal membrane folding, and numerous mitochondria. In the antennal gland, the main cell type is the continuous simple cuboidal labyrinthine (LBR). Arrows in (Fig. 4A', B') identify the width of the labyrinth lumen. In this study, results showed that the width of the labyrinth lumen of 5 ‰ group was more dilated to 103.57 ± 2.54 μm in comparison to 71.17 ± 6.8 μm of the 23 ‰ group (Fig. 4E). In addition, there were more mitochondria (8 ± 2) in the LBRs of the 5 ‰ group (black arrows in Fig. 4C and D) than those shown in 23 ‰ group (30 ± 8) (Fig. 4F).

### 3.4. The short-term adaptive responses to the sudden decline of salinity

Our result showed most mortality caused by the sudden decline of salinity took place within 24 h (Fig. S3). For the survived crabs, the hemolymph osmolality dropped from 824.0 ± 13.6 to 545.8 ± 27.6 mOsm/kg during the first 12 h and did not change afterwards (Fig. S4A); meanwhile, the environmental osmolality appeared to increase despite not being in a significant way. Accordingly, the concentration of Na^+, K^+, Mg^{2+} and Cl^- in the hemolymph decreased from 340.2 ± 4.9 to 203.5 ± 5.6 mmol/L (Fig. S4B), 6.8 ± 0.1 to 3.3 ± 0.1 mmol/L (Fig. S4D), 10.8 ± 0.1 to 7.0 ± 0.5 mmol/L (Fig. S4F), and 236.2 ± 4.9 to 203.5 ± 5.3 mmol/L (Fig. S4C); simultaneously, the environmental Na^+, K^+, Mg^{2+} and Cl^- increased from 147.0 ± 7.0 to 216.0 ± 8.0 mmol/L (Fig. S4B), 2.0 ± 0.2 to 3.3 ± 0.3 mmol/L (Fig. S4D), 4.7 ± 0.4 to 7.3 ± 0.5 mmol/L (Fig. S4F), 147.0 ± 7.0 to 222.7 ± 6.1 mmol/L (Fig. S4C). The new equilibrium of ion concentration between hemolymph and environment was achieved within 12–24 h.

The situation of Ca^{2+} was a bit different from that of other ions. In the 5 ‰ group, the hemolymph Ca^{2+} decreased from 9.9 ± 0.1 to 5.9 ± 0.1 mmol/L during the first 24 h and did not change afterwards; meanwhile, the environmental Ca^{2+} increased from 4.7 ± 0.2 to

Table 3
The sequence of primers used in RT-qPCR.

| Gene name	Primer sequence (5′→3′)
NBC1-qF	GATGGTGGGTGGCATAGTCAT
NBC1-qR	TGGATTGGAGTAGAAGAGGTGGT
NKA-qF	CCAGGATTGCTGCTCTTTG3
NKA-qR	CGGAAGCATCACCGTTTACC
NHE-qF	CCAGCCAGTGTCCAACAACA
NHE-qR	CCGAGGGTCAGCCTTCTTTT
VPA-qF	CCGTGGTCATGGCTGGTATC
VPA-qR	CCAGGTGGACAAAGCCGTAG
CA-g-qF	GCTGAAGCAGTGTGGTCGTA
CA-g-qR	TTCTCGAACACGAAGGGTGG
CA-c-qF	CAACCTCAGCCACGAAGACT
CA-c-qR	GGCCAAGTATCGGGACCATT
AC-qF	TCAAGGCAAGAGTGCAGGAT
AC-qR	TCTCCCCTGTGGTGTGTTGA
PEPCK-qF	AGCCGCTGCCCAAGTATAA
PEPCK-qR	CGTCACGATGAACGTCTTGC
SLC25-qF	GGCTCGTCACTTACCCCATC
SLC25-qR	CCACGCTGCTCTTGAGACAG
MDH-qF	ATCCGAGACTTTGCCCACTC
MDH-qR	TGTCCTTGAAACGTCCATCGT
SDH-qF	ACCGCCTCGTGAAGATTGTT
SDH-qR	TAGGAGTGTTGGGGCGTAGA
CFTR-qF	ATCATGCGCCTTGAGTCTGTC
CFTR-qR	TGCCTCTTGAATGCCCGTA
β-actin-qF	GCGGCAGTGGTCATCTCCT
β-actin-qR	GCCCTTCCTCACGCTATCCT
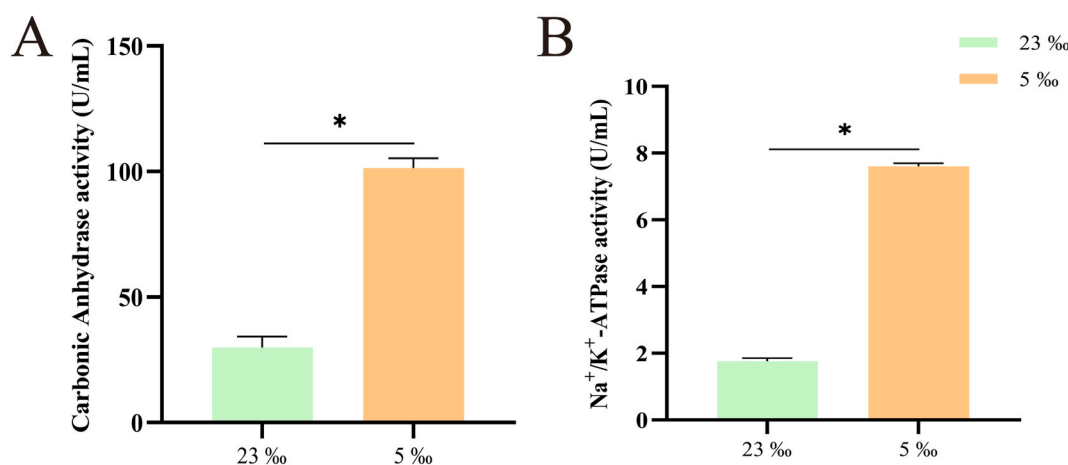
Fig. 3. The increased activity of two key enzymes related to ion transportation in the antennal glands of *S. paramamosain* as adapted to low salinity. A, the comparison of carbonic anhydrase activity between two groups; B, the comparison of Na^+/K^+-ATPase activity between two groups. Bars in the diagrams represent the mean $\pm$ SD, and statistically significant difference ($P < 0.05$) is indicated by an asterisk (*).

7.2 ± 0.3 mmol/L during the first 6 h. Unlike the cases of other ions, the environmental Ca^{2+} of the 23 ‰ group was not maintained at the initial level, it decreased from 8.0 ± 0.2 to 5.3 ± 0.3 mmol/L during the first 6 h and did not change afterwards (Fig. S4E).

During the short-term adaptation to low salinity, the enzyme of CA-c responded faster than NKA and the responsive period of CA-c was longer. The enzyme activity of CA rose immediately and reached peak after 48 h (Fig. 5A); in comparison, NKA enzyme activity increased 3 h after the salinity change while the level stabilized at 6 h, which was sooner than CA (Fig. 5B). The gene expression of *CA-c* (Fig. S5E) and *NKA* (Fig. S5B) showed a correspondingly changing pattern; nonetheless, a plummeted expression of *CA-c* was observed from 72 to 96 h (Fig. S5E).

Similar to *NKA*, the rising expression of *CFTR* (Fig. S5H), *SLC25* (Fig. S5I) and *PEPCK* (Fig. S5J) occurred within 24 h and the gene expression maintained at the peak level afterwards. For *VPA* (Fig. S5D) and *AC* (Fig. S5G), there was a temporary drop of the gene expression between 24 h and 72 h. For *NHE* (Fig. S5C), *MDH* (Fig. S5K) and *SDH* (Fig. S5L), the gene expression peaked at 24 h and started to fall afterwards. Unlike other genes, the expression of *NBC1* (Fig. S5A) and *CA-g* (Fig. S5F) began to decline since 0 h, rebound from 12 h to 24 h, then fell again.
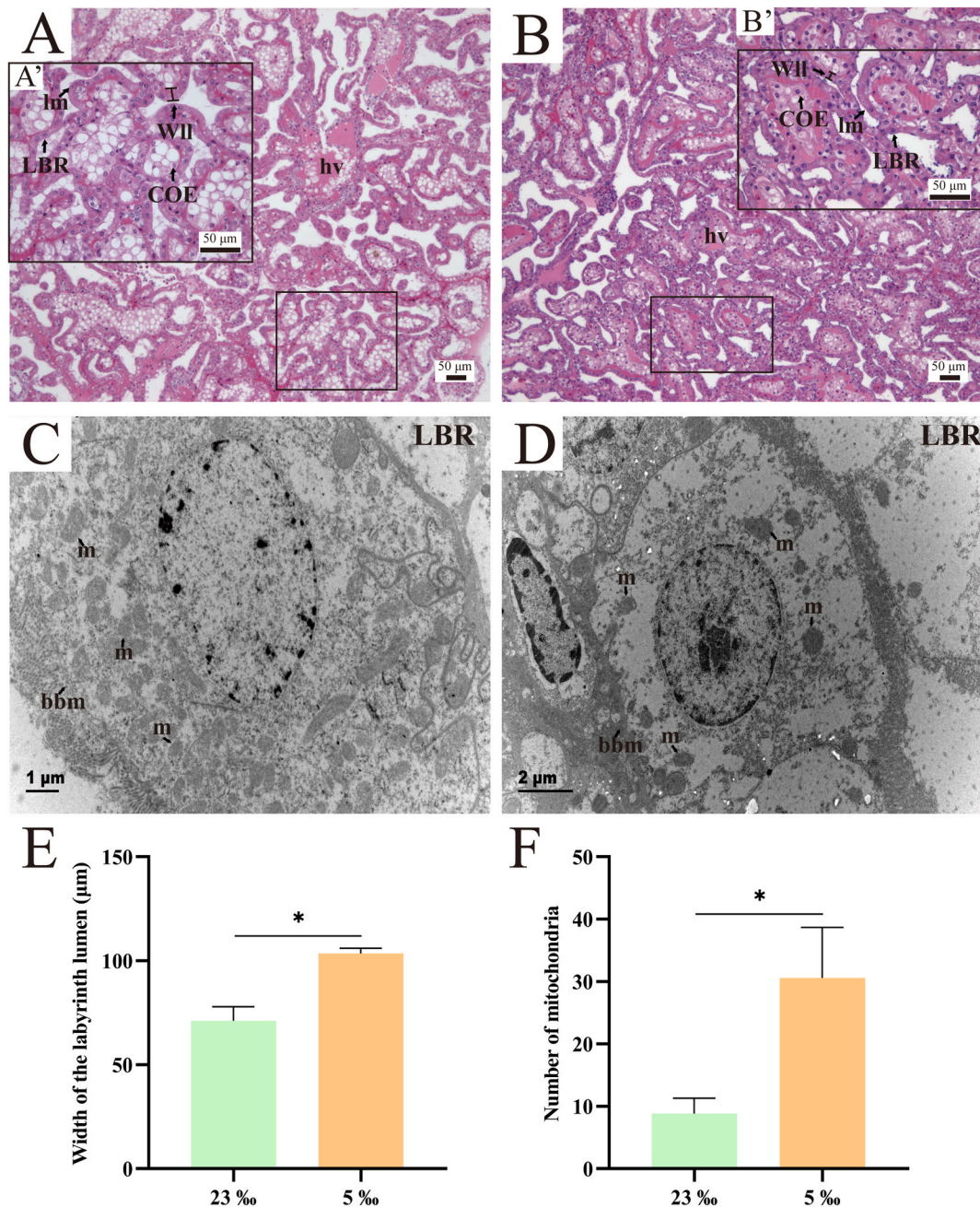
Fig. 4. The structural comparison of antennal glands between the 23 ‰ and 5 ‰ groups. A, A′ and C, the light and transmission electron microscopical images of the cross sections of the antennal glands of the 5 ‰ group. B, B′, and D, the light and transmission electron microscopical images of the cross sections of the antennal glands of the 23 ‰ group. E, the width of the labyrinth lumen (Wll). F, the number of mitochondria present in each LBRs cell. In section, the sectioning level is crossing through the anterior part and includes both proximal tubular region and distal tubular region. Tubular cells and large coelomosac are found in the peripheral of the antennal gland defined as distal tubular region. A large hemolymph vessel (hv) is found in the centre of the antennal gland which is defined as proximal tubular region. LBRs are cuboidal cells with apical brush-boarder microvilli (bbm), basolateral membrane folding and lots of mitochondria (m). Scale bars: 50 μm (A, A′, B, B′), 1 μm (C), 2 μm (D).

4. Discussion

Our results showed that the pathways of ion regulation including "proximal tubule bicarbonate reclamation" and "mineral absorption" were activated in the antennal glands of *S. paramamosain* during the adaptation to low salinity. The genes for the ion transporters, e.g. *NKA*, *CA-c*, *VPA* and *NHE*, were up-regulated. The increase of enzyme activities of NKA and CA-c confirmed the
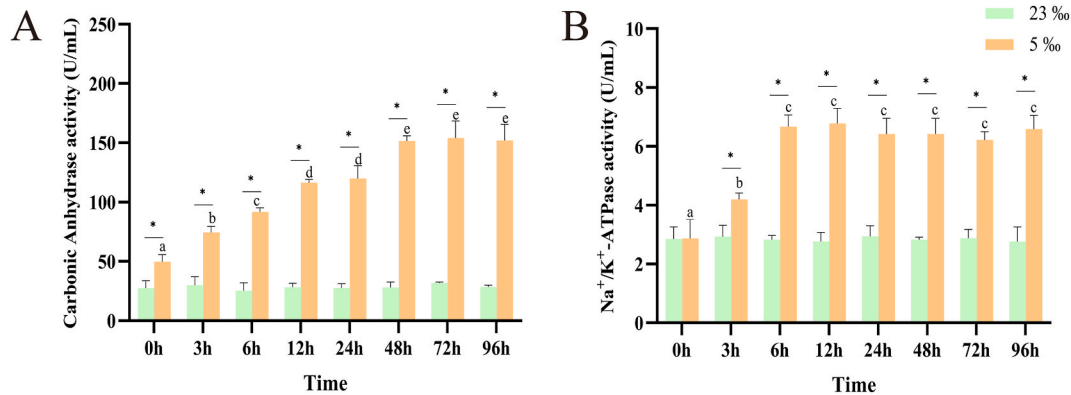
Fig. 5. The effect of a sudden decline of salinity on the activity of two key ion transportation enzymes in the antennal glands of *Scylla paramamosain*. A, the change of carbonic anhydrase activity over 96 h; B, the change of Na^+/K^+-ATPase activity over 96 h. Bars represent the mean ± SD, statistically significant differences ($P < 0.05$) are indicated by an asterisk (*).

activation of these two genes. *NKA* is a membrane-associated enzyme responsible for transporting K^+ in and Na^+ out of the cell [23]. *NHE* is also a membrane protein which transports Na^+ in and H^+ out [62]. *VPA* can transport H^+ across the plasma membrane [37]. CA catalyzes the bidirectional conversion of H_2O and CO_2 to H^+ and HCO_3^-, where H^+ is often provided for other ion transporters [43].

The upregulation of *AC* might be related to the activation of AC-cAMP-PKA-ion transporter signaling pathway [63], which has been suggested as a crucial signal transduction pathway regulated by the crustacean neuroendocrine system [[64–66]]. It has been shown that cAMP mediated neuroendocrine factors play important roles in the crustacean osmoregulation [[67–69]]. In crustaceans, the gills are primarily responsible for osmoregulation, which involves efficient ion transport, regulation of hemolymph, and changes in metabolism through increased O_2 consumption to regulate hemolymph ion concentration [16,17,38]. These results showed the osmoregulatory function of antennal glands depends on the ionic reabsorption via the activation of ion transporters (Fig. 6). The response mechanisms of the gill and antennal glands may differ, and osmoregulation homeostasis is regulated by the coordinated action of gill and antennal glands. However, the deficiency is that we did not find differences in the response of genes related to osmotic regulation during long-term and short-term low-salt adaptation, which may be because only a few selected genes were detected for long-term and short-term exposure.

Our study also found that the expression of genes associated with energy reallocation is orchestrated in the antennal gland in response to low salinity. *SDH* and *MDH* are critical enzymes in the TCA cycle [70]. *PEPCK* converts oxaloacetate (OAA) to phosphoenolpyruvate (PEP) during gluconeogenesis [[71–73]]. *SLC25* mediates the translocation of substances including amino acids, sugars, and inorganic ions across mitochondrial membrane [74]. The upregulation of *MDH*, *SLC25* and *PEPCK* and the downregulation of *SDH* implied the enhancement of gluconeogenesis (Fig. 6). This result was consistent with the observation of increased mitochondria in the luminal podocytes of the antennal gland in response to low salinity. It was possibly related to the requirement of extra energy from non-carbohydrate resources as a way of metabolic reprogramming for the intensive osmoregulation during low salinity adaptation [[75–77]].

Our results showed that the hemolymph osmolality and the hemolymph concentrations of Na^+, Cl^-, Ca^{2+}, Mg^{2+} and K^+ decreased as adapted to the low salinity, and eventually the internal osmolality equilibrates to a steady state with the external ambient osmolality. After a sudden drop in salinity, the hemolymph osmolality of *S. paramamosain* balance to the environmental osmolality within 12–24 h. O_2 consumption, increased energy requirements and accelerated metabolism due to changes in salinity lead to physiological dysfunction and reduced immune defense capacity, as most mortality was also observed during the same period. Another study also observed a lowered hemolymph osmolality of *S. paramamosain* reared in low salinity water [6]. In contrast, an increase in hemolymph osmolality was observed in the freshwater crab *Eriocheir sinensis* when accumulated in a high salinity environment [78]. As a result, crabs such as *S. paramamosain* and *E. sinensis* are also known to be strong osmoregulator, maintaining hemolymph osmolality very similar to that of the external environment. *E. sinensis* mainly live in fresh water while *S. paramamosain* and *P. trituberculatus* are estuaries or ocean dwelling [[25,37,38]]. The change of salinity is one of the important factors that directly affect the occupation of crustaceans to the environment [52,61]. For crustaceans, osmotic balance in low or high salinity is achieved by transport mechanisms, osmotic and ionic regulation [43,62]. Successfully occupying environments of different salinity requires the ability to respond quickly to changes in salinity.

Based on our cross section of the antennal gland, this explains the enlarged labyrinthic lumen inside the antennal gland observed in this and other studies during low salinity adaptation [79,80]. Low osmolality external water is likely to penetrate high osmolality hemolymph and dilute the hemolymph. To compensate for the increased volume of hemolymph, excess water is excreted through the antennal glands as low osmolality urine.

In summary, our study has revealed the osmoregulatory function of the antennal glands of *S. paramamosain* via the findings of upregulation of the ion-transporter gene, deactivation of the enzyme activity of the ion-transporter, and rebalancing of hemolymph osmolality as the crab adapts to low salinity. For low salinity adaptations, crabs increase excretion of urine and ionic reabsorption from urine in the antennal glands. Additionally, we found that crabs occupying an environment of changing salinity may require additional
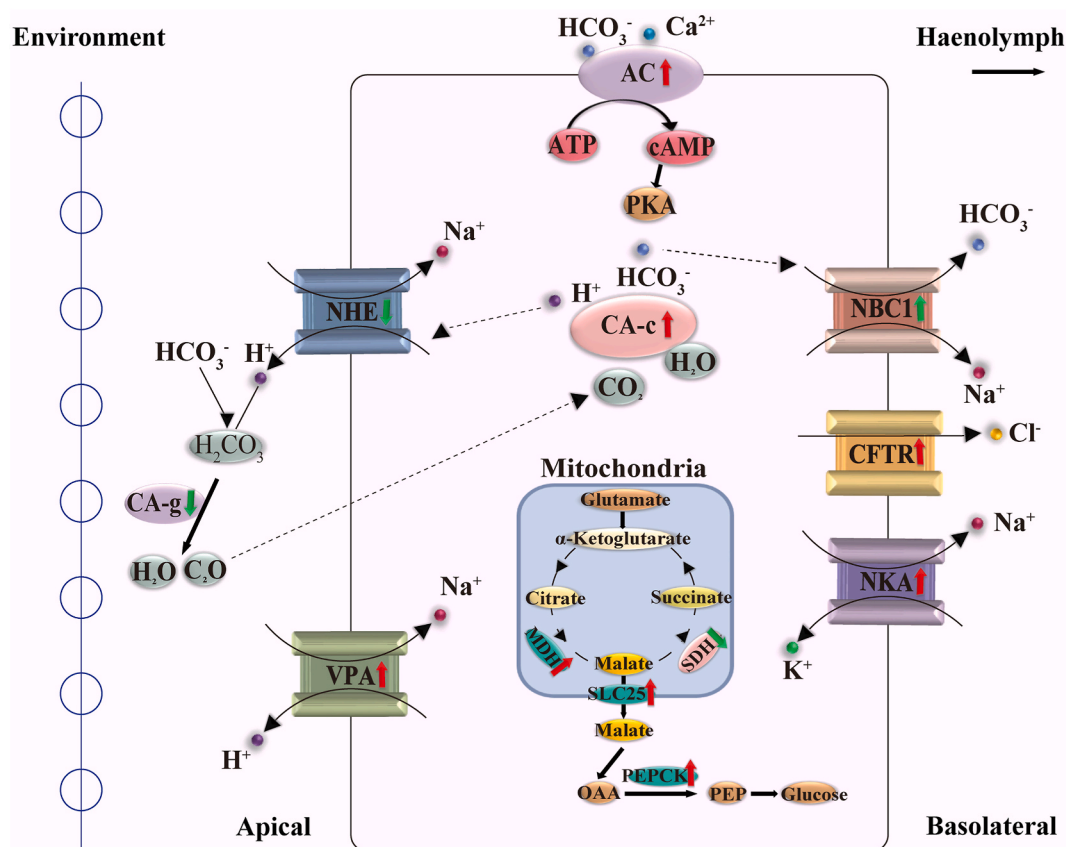
Fig. 6. The proposed osmoregulatory pathway of antennal glands of *S. paramamosain* as adapted to low salinity. Red arrows indicate gene up-regulation and green arrows indicate gene down-regulation. *NBC1*, solute carrier family 1; *NKA*, Na$^+$/K$^+$-ATPase; *NHE*, sodium/hydrogen exchanger; *VPA*, V-type proton (H$^+$)-ATPase; *CA-g*, glycosyl-phosphatidylinositol-linked carbonic anhydrase; *CA-c*, cytoplasmic carbonic anhydrase; *AC*, adenylate cyclase; *CFTR*, ATP-binding cassette, subfamily C; *SLC25*, solute carrier family 25; *PEPCK*, phosphoenolpyruvate carboxykinase; *MDH*, malate dehydrogenase; *SDH*, succinate dehydrogenase.

energy expenditure to carry out transport mechanisms and osmotic and ionic regulation. It is necessary to acknowledge the limitations of this work. The only few selected genes we used to experimentally validate were examined for both long- and short-term exposures, the qPCR results might not reflect the global responses and expression profile in mud crab. Future research with larger scale is needed.

Data availability statement

The sample data used in this article has been submitted to the NCBI SRA database (Bioproject：PRJNA881792). Upon reasonable request, the datasets used and analyzed during the present study are also available from the corresponding author.

Institutional review board statement

The committee on the Ethics of Animal Experiments of Ningbo University (No. SYXK20190005) was established in 2019, but the committee authorities were only for rabbits, mice, and rats, and not aquatic animals. In this study, mature and juvenile crabs were purchased from commercial farms, and all experimental operations involving animals complied with the requirements of the governing regulation for the use of experimental animals in Zhejiang Province (Zhejiang provincial government order No. 263, released on August 17, 2009, effective from October 1, 2010) and were performed according to the Experimental Animal Management Law of China and met the animal operation standards of the industry.

CRediT authorship contribution statement

Nan Mo: Writing – review & editing, Writing – original draft, Visualization, Validation, Methodology, Investigation, Data curation. **Tianyi Feng:** Writing – review & editing, Supervision, Formal analysis. **Dandan Zhu:** Methodology. **Jiaxin Liu:** Visualization, Methodology. **Shucheng Shao:** Methodology. **Rui Han:** Methodology. **Wentao Lu:** Methodology. **Pingping Zhan:** Visualization, Methodology. **Zhaoxia Cui:** Writing – review & editing, Supervision, Resources, Project administration, Funding acquisition, Conceptualization.

Declaration of competing interest

The authors declare that they have no known competing financial interests or personal relationships that could have appeared to influence the work reported in this paper.

Acknowledgments

Appendix A. Supplementary data

Supplementary data to this article can be found online at https://doi.org/10.1016/j.heliyon.2024.e25556.

References

[1] K. Anger, Salinity tolerance of the larvae and first juveniles of a semiterrestrial grapsid crab, *Armases miersii* (Rathbun), J. Exp. Mar. Biol. Ecol. 202 (2) (1996) 205–223, https://doi.org/10.1016/0022-0981(96)00022-6.

[2] K. Anger, Salinity as a key parameter in the larval biology of decapod crustaceans, Invertebr. Reprod. Dev. 43 (1) (2003) 29–45, https://doi.org/10.1080/07924259.2003.9652520.

[3] B.K. Chand, R.K. Trivedi, S.K. Dubey, S.K. Rout, M.M. Beg, U.K. Das, Effect of salinity on survival and growth of giant freshwater prawn *Macrobrachium rosenbergii* (de man), Aquaculture Reports 2 (C) (2015) 26–33, https://doi.org/10.1016/j.aqrep.2015.05.002.

[4] D. Huong, V. Jayasankar, S. Jasmani, H. Saido-Sakanaka, A.J. Wigginton, M.N. Wilder, Na/K-ATPase activity during larval development in the giant freshwater prawn *Macrobrachium rosenbergii* and the effects of salinity on survival rates, Fisheries Science 70 (3) (2010) 518–520, https://doi.org/10.1111/j.1444-2906.2004.00833.x.

[5] M.S. Shekhar, J. Kiruthika, A.G. Ponniah, Identification and expression analysis of differentially expressed genes from shrimp (*Penaeus monodon*) in response to low salinity stress, Fish Shellfish Immunol. 35 (6) (2013) 1957–1968, https://doi.org/10.1016/j.fsi.2013.09.038.

[6] J. Zhou, N. Li, H. Wang, C.K. Mu, C.L. Wang, Effects of salinity on the ions important and sodium-potassium ATPase in osmoregulation, cortisol, amino acids, digestive and immune enzymes in *Scylla paramamosain* during indoor overwintering, Aquacult. Res. 51 (2020) 4173–4182, https://doi.org/10.1111/are.14759.

[7] E.C. Li, L.Q. Chen, C. Zeng, X.M. Chen, N. Yu, Q.M. Lai, J.G. Qin, Growth, body composition, respiration and ambient ammonia nitrogen tolerance of the juvenile white shrimp, *litopenaeus vannamei*, at different salinities, Aquaculture 265 (1–4) (2007) 385–390, https://doi.org/10.1016/j.aquaculture.2007.02.018.

[8] L. Pan, D. Hu, M. Liu, Y. Hu, S. Liu, Molecular cloning and sequence analysis of two carbonic anhydrase in the swimming crab *Portunus trituberculatus* and its expression in response to salinity and pH stress, Gene 576 (1P2) (2015) 347–357, https://doi.org/10.1016/j.gene.2015.10.049.

[9] N. Romano, C. Zeng, Importance of balanced Na^+/K^+ ratios for blue swimmer crabs, *Portunus pelagicus*, to cope with elevated ammonia-N and differences between in vitro and in vivo gill Na^+/K^+-ATPase responses, Aquaculture 318 (1–2) (2011) 154–161, https://doi.org/10.1016/j.aquaculture.2011.05.016.

[10] R.P. Henry, S. Gehnrich, D. Weihrauch, D.W. Towle, Salinity-mediated carbonic anhydrase induction in the gills of the euryhaline green crab, *Carcinus maenas*, Comp. Biochem. Physiol. Mol. Integr. Physiol. 136 (2) (2003) 243–258, https://doi.org/10.1016/S1095-6433(03)00113-2.

[11] L.M. Ji, P.D. Trausch, Active absorption of Cl^- and Na^+ in posterior gills of Chinese crab *Eriocheir sinensis*: modulation by dopamine and cAMP, J. Crustac Biol. 23 (3) (2003) 505–512, https://doi.org/10.2307/1549882.

[12] S. Morris, Neuroendocrine regulation of osmoregulation of osmoregulation and the evolution of air breathing in decapod crustaceans, J. Exp. Biol. 204 (5) (2001) 979–989, https://doi.org/10.1002/nau.20194.

[13] M. Rathmayer, D. Siebers, Ionic balance in the freshwater-adapted Chinese crab, *Eriocheir sinensis*, J. Comp. Physiol. B 171 (4) (2001) 271–281, https://doi.org/10.1007/s003600100173.

[14] X.L. Han, L. Ping, B.Q. Gao, H.F. Wang, Y.F. Duan, W.F. Xu, P. Chen, Na^+/K^+-ATPase α-subunit in swimming crab *Portunus trituberculatus*: molecular cloning, characterization, and expression under low salinity stress, Chin. J. Oceanol. Limnol. 33 (2015) 828–837, https://doi.org/10.1007/s00343-015-4018-9.

[15] S. Chapelleo, Influence of salinity on the lipid composition and the fatty-acid pattern of muscle and hepatopancreas of the Chinese crab *Eriocheir sinensis*, Arch. Int. Physiol. 86 (2) (2008) 393–401, https://doi.org/10.3109/13813457809069914.

[16] R.P.M. Furriel, K.C.S. Firmino, D.C. Masui, R.O. Faleiros, A.H. Torres, J.C. McNamara, Structural and biochemical correlates of Na^+, K^+-ATPase driven ion uptake across the posterior gill epithelium of the true freshwater crab, *Dilocarcinus pagei* (Brachyura, Trichodactylidae), J. Exp. Zool. 313A (2010) 508–523, https://doi.org/10.1002/jez.622.

[17] J.C. McNamara, C.A. Freire, A.H. Torres, S.C. Faria, The conquest of fresh water by palaemonid shrimps: an evolutionary history scripted in the osmoregulatory epithelia of the gills and antennal glands, Biological Journal of the Linnaean Society 114 (3) (2015) 673–688, https://doi.org/10.1111/bij.12443.

[18] C.L. Negro, Histopathological effects of endosulfan to hepatopancreas, gills and ovary of the freshwater crab *Zilchiopsis collastinensis* (Decapoda: Trichodactylidae), Ecotoxicol. Environ. Saf. 113 (2015) 87–94, https://doi.org/10.1016/j.ecoenv.2014.11.025.

[19] D. Sun, J. Lv, B. Gao, P. Liu, J. Li, Crustacean hyperglycemic hormone of *Portunus trituberculatus*: evidence of alternative splicing and potential roles in osmoregulation, Cell Stress Chaperones 24 (3) (2019) 517–525, https://doi.org/10.1007/s12192-019-00980-6.

[20] H. Onken, M. Putzenlechner, A V-ATPase drives active, electrogenic and Na^+-independent Cl^- absorption across the gills of *Eriocheir sinensis*, J. Exp. Biol. 198 (Pt 3) (1995) 767–774, https://doi.org/10.1242/jeb.198.3.767, 1995.

[21] D. Weihrauch, A. Ziegler, D. Siebers, D.W. Towle, Active ammonia excretion across the gills of the green shore crab *Carcinus maenas*: participation of Na^+/K^+-ATPase, V-type H^+-ATPase and functional microtubules, J. Exp. Biol. 205 (2002) 2765–2775, https://doi.org/10.1242/JEB.205.18.2765.

[22] J. Lv, P. Liu, Y. Wang, B. Gao, P. Chen, J. Li, Transcriptome analysis of *Portunus trituberculatus* in response to salinity stress provides insights into the molecular basis of osmoregulation, PLoS One 8 (12) (2013) e82155, https://doi.org/10.1371/journal.pone.0082155.

[23] F.A. Leone, D.P. Garçon, M.N. Lucena, R.O. Faleiros, S.V. Azevedo, M.R. Pinto, J.C. McNamara, Gill-specific (Na$^+$, K$^+$)-ATPase activity and alpha-subunit mRNA expression during low-salinity acclimation of the ornate blue crab *Callinectes ornatus* (Decapoda, Brachyura). Comparative biochemistry and physiology, Part B, Biochemistry & molecular biology 186B (2015) 59–67, https://doi.org/10.1016/j.cbpb.2015.04.010.

[24] J.J. Lv, D. Sun, D. Yan, X. Ti, P. Liu, J. Li, Quantitative trait loci mapping and marker identification for low salinity tolerance trait in the swimming crab (*Portunus trituberculatus*), Front. Genet. 10 (2019) 1193, https://doi.org/10.3389/fgene.2019.01193.

[25] M. Reuter, M.F. Camus, M.S. Hill, F. Ruzicka, K. Fowler, Evolving plastic responses to external and genetic environments, Trends Genet. 33 (3) (2017) 169–170, https://doi.org/10.1016/j.tig.2017.01.004.

[26] N. Romano, C. Zeng, Survival, osmoregulation and ammonia-N excretion of blue swimmer crab, *Portunus pelagicus*, juveniles exposed to different ammonia-N and salinity combinations, Comp. Biochem. Physiol. C Toxicol. Pharmacol. 151 (2) (2010) 222–228, https://doi.org/10.1016/j.cbpc.2009.10.011.

[27] Z. Sheng, M.E. Pettersson, C.F. Honaker, P.B. Siegel, Ö. Carlborg, Standing genetic variation as a major contributor to adaptation in the Virginia chicken lines selection experiment, Genome Biol. 16 (2015) 219, https://doi.org/10.1186/s13059-015-0785-z.

[28] G.A. Wray, Genomics and the evolution of phenotypic trait, Annu. Rev. Ecol. Evol. Systemat. 44 (2013) 51–72, https://doi.org/10.1146/annurev-ecolsys-110512-135828.

[29] M.C. De Vries, D.L. Wolcott, C.W. Holliday, High ammonia and low pH in the urine of the ghost crab, *Ocypode quadrata*, Biol. Bull. 186 (3) (1994) 342–348, https://doi.org/10.2307/1542280.

[30] S. Morris, M.D. Ahern, Regulation of urine reprocessing in the maintenance of sodium and water balance in the terrestrial Christmas Island red crab *Gecarcoidea natalis* investigated under field conditions, J. Exp. Biol. 206 (Pt 16) (2003) 2869–2881, https://doi.org/10.1242/jeb.00499.

[31] M.G. Wheatly, The role of the antennal gland in ion and acid-base regulation during hyposaline exposure of the Dungeness crab Cancer magister (Dana), J. Comp. Physiol. B 155 (4) (1985) 445–454, https://doi.org/10.1007/BF00684674.

[32] D. Brown, T.G. Paunescu, S. Breton, V. Marshansky, Regulation of the V-ATPase in kidney epithelial cells: dual role in acid-base homeostasis and vesicle trafficking, J. Exp. Biol. 212 (2009) 1762–1772, https://doi.org/10.1242/jeb.028803.

[33] A.P.M. Lockwood, J.A. Riegel, The excretion of magnesium by *Carcinus maenas*, J. Exp. Biol. 51 (1969) 575–589, https://doi.org/10.1242/jeb.51.3.575.

[34] K.Y. Tseng, J.R. Tsai, H.C. Lin, Ion regulation in the antennal glands differs among Ocypodoidea and Grapsoidea crab species, Comp. Biochem. Physiol. Part A Molecular & Integrative Physiology 248 (2020) 110753, https://doi.org/10.1016/j.cbpa.2020.110753.

[35] L.H. Mantel, L.L. Farmer, Osmotic and ionic regulation, in: L.H. Mantel (Ed.), The Biology of the Crustacean, Internal Anatomy and Physiological Regulation, vol. 5, 1983, pp. 53–161, https://doi.org/10.1146/annurev.ph.30.030160.000445.

[36] C.A. Freire, H. Onken, J.C. Mcnamara, A structure-function analysis of ion transport in crustacean gills and excretory organs, Comp. Biochem. Physiol. Part A Molecular & Integrative Physiology 151 (3) (2008) 272–304, https://doi.org/10.1016/j.cbpa.2007.05.008.

[37] J.R. Tsai, H.C. Lin, Functional anatomy and ion regulatory mechanisms of the antennal gland in a semi-terrestrial crab, *Ocypode stimpsoni*, Biology Open 3 (6) (2014) 409–417, https://doi.org/10.1242/bio.20147336.

[38] H.Z. Yao, X. Li, L. Tang, H. Wang, C.K. Mu, C.L. Wang, C. Shi, Metabolic mechanism of the mud crab (*Scylla paramamosain*) adapting to salinity sudden drop based on GC-MS technology, Aquaculture Reports 18 (2020) 100533, https://doi.org/10.1016/j.aqrep.2020.100533.

[39] J.A. Riegel, Micropuncture studies of chloride concentration and osmotic pressure in the crayfish antennal gland, J. Exp. Biol. 40 (1963) 487–492, https://doi.org/10.1242/jeb.40.3.487.

[40] D.R. Peterson, R.F. Loizzi, Regional cytology and cytochemistry of the crayfish kidney tubule, J. Morphol. 141 (1973) 133–145, https://doi.org/10.1002/jmor.1051410202.

[41] D.R. Peterson, R.F. Loizzi, Ultrastructure of the crayfish kidney coelomosac, labyrinth, nephridial canal, J. Morphol. 142 (1974) 241–263, https://doi.org/10.1002/jmor.1051420302.

[42] R.P. Henry, Environmentally mediated carbonic anhydrase induction in the gills of euryhaline crustaceans, J. Exp. Biol. 204 (2001) 991–1002, https://doi.org/10.1242/jeb.204.5.991.

[43] R.P. Henry, C. Lucu, H. Onken, D. Weihrauch, Multiple functions of the crustacean gill: osmotic/ionic regulation, acid-base balance, ammonia excretion, and bioaccumulation of toxic metals, Front. Physiol. 3 (431) (2012) 1–33, https://doi.org/10.3389/fphys.2012.00431.

[44] D. Weihrauch, Ammonia excretion in aquatic and terrestrial crabs, J. Exp. Biol. 207 (26) (2004) 4491–4504, https://doi.org/10.1242/jeb.01308.

[45] G. Charmantier, M. Charmantier-Daures, D. Towle, Osmotic and ionic regulation in aquatic arthropods, in: D.H. Evans (Ed.), Osmotic and Ionic Regulation: Cells and Animals, CRC Press, Boca Raton, 2008, pp. 165–230, https://doi.org/10.1201/9780849380525-6.

[46] W. Jiang, H.Y. Ma, C.Y. Ma, S.J. Li, Y.X. Liu, Z.G. Qiao, L.B. Ma, Characteristics of growth traits and their effects on body weight of g₁ individuals in the mud crab (*Scylla paramamosain*), Genet. Mol. Res. 13 (3) (2014) 6050–6059, https://doi.org/10.4238/2014.August.7.19.

[47] M. Zhao, W. Wang, C. Ma, F. Zhang, L. Ma, Characterization and expression analysis of seven putative JHBPs in the mud crab *Scylla paramamosain*: putative relationship with methyl farnesoate, Comp. Biochem. Physiol. B Biochem. Mol. Biol. 241 (2020) 110390, https://doi.org/10.1016/j.cbpb.2019.110390.

[48] Y. Dai, K. Han, Z. Zou, S. Yan, Y. Wang, Z. Zhang, SUMO-1 of mud crab (*Scylla paramamosain*) in gametogenesis, Gene 503 (2) (2012) 260–268, https://doi.org/10.1016/j.gene.2012.04.056.

[49] H.Z. Yao, X. Li, Y.H. Chen, G.L. Liang, G. Gao, H. Wang, C.K. Mu, C.L. Wang, Metabolic changes in *Scylla paramamosain* during adaptation to an acute decrease in salinity, Front. Mar. Sci. (2021) 734519, https://doi.org/10.3389/fmars.2021.734519.

[50] H. Wang, H. Wei, L. Tang, J. Lu, C.K. Mu, C.L. Wang, Identification and characterization of miRNAs in the gills of the mud crab (*Scylla paramamosain*) in response to a sudden drop in salinity, BMC Genom. 19 (1) (2018) 609, https://doi.org/10.1186/s12864-018-4981-6.

[51] H. Wang, H. Wei, T. Lei, J. Lu, C.K. Mu, C.L. Wang, A proteomics of gills approach to understanding salinity adaptation of *Scylla paramamosain*, Gene 677 (2018) 119–131, https://doi.org/10.1016/j.gene.2018.07.059.

[52] H. Wang, T. Lei, H. Wei, J. Lu, C.K. Mu, C.L. Wang, Transcriptomic analysis of adaptive mechanisms in response to sudden salinity drop in the mud crab, *Scylla paramamosain*, BMC Genom. 19 (1) (2018) 421, https://doi.org/10.1186/s12864-018-4803-x.

[53] J. Du, Y. Liu, C.W. Song, Z.X. Cui, Discovery of sex-related genes from embryonic development stage based on transcriptome analysis in *Eriocheir sinensis*, Gene 710 (2019) 1–8, https://doi.org/10.1016/j.gene.2019.05.021.

[54] P.J. Cock, C.J. Fields, N. Goto, M.L. Heuer, P.M. Rice, The Sanger FASTQ file format for sequences with quality scores, and the Solexa/Illumina FASTQ variants, Nucleic Acids Res. 38 (6) (2010) 1767–1771, https://doi.org/10.1093/nar/gkp1137.

[55] S. Anders, W. Huber, Differential expression analysis is for sequence count data, Genome Biol. 11 (10) (2010) R106, 10.1038/npre.2010.4282.1.

[56] D. Kim, B. Langmead, S.L. Salzberg, HISAT: a fast spliced aligner with low memory requirements, Nat. Methods 12 (2015) 357–360, https://doi.org/10.1038/nmeth.3317.

[57] A.V. Boyko, A.S. Girich, M.G. Eliseikina, S.I. Maslennikov, I.Y. Dolmatov, Reference assembly and gene expression analysis of *Apostichopus japonicus* larval development, Sci. Rep. 9 (1) (2019) 1131, https://doi.org/10.1038/s41598-018-37755-5.

[58] A. Conesa, S. Gotz, J.M. Garcia-Gomez, J. Terol, M. Talón, M.Blast2GO. Robles, A universal tool for annotation, visualization and analysis in functional genomics research, Bioinformatics 21 (18) (2005) 3674–3676, https://doi.org/10.1093/bioinformatics/bti610.

[59] M. Kanehisa, S. Goto, S. Kawashima, Y. Okuno, M. Hattori, The KEGG resource for deciphering the genome, Nucleic Acids Res. 32 (2004) D277–D280, https://doi.org/10.1093/nar/gkh063.

[60] T.D. Schmittgen, Analyzing real-time PCR data by the comparative CT method, Nat. Protoc. (2008), https://doi.org/10.1038/nprot.2008.73.

[61] X. Long, X. Wu, L. Zhao, H. Ye, Y. Cheng, C. Zeng, Effects of salinity on gonadal development, osmoregulation and metabolism of adult male Chinese mitten crab, *Eriocheir sinensis*, PLoS One 12 (6) (2017) e0179036, https://doi.org/10.1371/journal.pone.0179036.

[62] R.E. Shetlar, D.W. Towle, Electrogenic sodium-proton exchange in membrane vesicles from crab (*Carcinus maenas*) gill, Am. J. Physiol. 257 (4 Pt 2) (1989) R924–R931, https://doi.org/10.1111/j.1748-1716.1989.tb08758.x.

[63] H. Yang, X. He, J. Yang, X. Deng, Y. Liao, Z. Zhang, C. Zhu, Y. Shi, N. Zhou, Activation of cAMP-response element-binding protein is positively regulated by PKA and calcium-sensitive calcineurin and negatively by PKC in insect, Insect Biochem. Mol. Biol. 43 (11) (2013) 1028–1036, https://doi.org/10.1016/j.ibmb.2013.08.011.

[64] J.L. Mo, P. Devos, G. Trausch, Dopamine D_1 receptors in the gills of Chinese crab *Eriocheir sinensis*, Comp. Biochem. Physiol. C Toxicol. Pharmacol. 131 (2002) 433–438, https://doi.org/10.1016/S1532-0456(02)00032-7.

[65] H. Liu, L. Pan, D. Zheng, Effects of injection of biogenic amines on expression of gill related ion transporter mRNA and α-subunit protein in *Litopenaeus vannamei*, Comp. Biochem. Physiol. Part A Molecular & Integrative Physiology 154 (2009) 29–36, https://doi.org/10.1016/j.cbpa.2009.01.004.

[66] A.E. Christie, E.A. Stemmler, P.S. Dickinson, Crustacean neuropeptides, Cell. Mol. Life Sci. 67 (24) (2010) 4135–4169, https://doi.org/10.1007/s00018-010-0482-8.

[67] M.C. Clark, D.J. Baro, Arthropod D_2 receptors positively couple with cAMP through the Gi/o protein family, Comp. Biochem. Physiol. B Biochem. Mol. Biol. 146 (1) (2007) 9–19, https://doi.org/10.1016/j.cbpb.2006.08.018.

[68] M.C. Clark, R. Khan, D.J. Baro, Crustacean dopamine receptors: localization and G protein coupling in the stomatogastric ganglion, J. Neurochem. 104 (4) (2008) 1006–1019, https://doi.org/10.1111/j.1471-4159.2007.05029.x.

[69] L. Xu, L. Pan, X. Zhang, C. Wei, Effects of crustacean hyperglycemic hormone (CHH) on regulation of hemocyte intracellular signaling pathways and phagocytosis in white shrimp *Litopenaeus vannamei*, Fish Shellfish Immunol. 93 (2019) 559–566, https://doi.org/10.1016/j.fsi.2019.07.051.

[70] A.R. Fernie, F. Carrari, L.J. Sweetlove, Respiratory metabolism: glycolysis, the TCA cycle and mitochondrial electron transport, Curr. Opin. Plant Biol. 7 (2004) 254–261, https://doi.org/10.1016/j.pbi.2004.03.007.

[71] Y. Ye, Y. An, R. Li, C.K. Mu, C.L. Wang, Strategy of metabolic phenotype modulation in *Portunus trituberculatus* exposed to low salinity, J. Agric. Food Chem. 62 (15) (2014) 3496–3503, https://doi.org/10.1021/jf405668a.

[72] D. Zhang, F. Wang, S. Dong, Y. Lu, De novo assembly and transcriptome analysis of osmoregulation in *Litopenaeus vannamei* under three cultivated conditions with different salinities, Gene 578 (2) (2016) 185–193, https://doi.org/10.1016/j.gene.2015.12.026.

[73] B. Sutherland, S.G. Jantzen, M. Yasuike, D.S. Sanderson, B.F. Koop, S.R. Jones, Transcriptomics of coping strategies in free-swimming *Lepeophtheirus salmonis* (copepoda) larvae responding to abiotic stress, Mol. Ecol. 21 (24) (2012) 6000–6014, https://doi.org/10.1111/mec.12072.

[74] F. Palmieri, P. Scarcia, M. Monné, Diseases caused by mutations in mitochondrial carrier genes SLC25: a review, Biomolecules 10 (4) (2020) 655, https://doi.org/10.3390/biom10040655.

[75] E. Li, S. Wang, C. Li, X. Wang, K. Chen, L. Chen, Transcriptome sequencing revealed the genes and pathways involved in salinity stress of Chinese mitten crab, *Eriocheir sinensis*, Physiol. Genom. 46 (5) (2014) 177–190, https://doi.org/10.1152/physiolgenomics.00191.2013.

[76] M. Hui, Y. Liu, C. Song, Y. Li, G. Shi, Z. Cui, Transcriptome changes in *Eriocheir sinensis* megalopae after desalination provide insights into osmoregulation and stress adaption in larvae, PLoS One 9 (2014) e114187, https://doi.org/10.1371/journal.pone.0114187.

[77] J.C. Havird, R.T. Mitchell, R.P. Henry, S.R. Santos, Salinity-induced changes in gene expression from anterior and posterior gills of *Callinectes sapidus* (Crustacea: portunidae) with implications for crustacean ecological genomics, Comp. Biochem. Physiol. Genom. Proteonomics 19 (2016) 34–44, https://doi.org/10.1016/j.cbd.2016.06.002.

[78] Z. Yang, J. Zhou, B. Wei, Y. Cheng, L. Zhang, X. Zhen, Comparative transcriptome analysis reveals osmotic-regulated genes in the gill of Chinese mitten crab (*Eriocheir sinensis*), PLoS One 14 (1) (2019) e0210469, https://doi.org/10.1371/journal.pone.0210469.

[79] S.C. Lin, C.H. Liou, J.H. Cheng, The role of the antennal glands in ion and body volume regulation of cannulated *Penaeus monodon* reared in various salinity conditions, Comp. Biochem. Physiol. Part A Molecular & Integrative Physiology 127 (2) (2000) 121–129, https://doi.org/10.1016/S1095-6433(00)00245-2.

[80] D. Buranajitpirom, S. Asuvapongpatana, W. Weerachatyanukul, K. Wongprasert, W. Namwong, P. Poltana, B. Withyachumnarnkul, Adaptation of the black tiger shrimp, *Penaeus monodon*, to different salinities through an excretory function of the antennal gland, Cell Tissue Res. 340 (3) (2010) 481–489, 10.1007/s00441-010-0971-y.